Article

High Performance Polymers

High Performance Polymers
24(8) 702–709

DOI: 10.1177/0954008312449846
hip.sagepub.com
SAGE

Enhanced toughness and shape memory behaviors of toughed epoxy resin

Chun-Hua Zhang[1], Hui-Ge Wei[1], Yu-Yan Liu[1,2], Hui-Feng Tan[2,3], and Zhanhu Guo[4]

Abstract

This paper reports on an approach to enhance the toughness of shape memory epoxy by using polypropylene glycol diglycidyl ether (G) as the toughening agent. The mechanical properties and shape memory behavior of the toughened resin systems with different loading level of G were studied, respectively. Results of the torsional braid analysis (TBA) test indicated that G had good compatibility with the epoxy resin matrix and induced a decrease in the glass transition temperature, T_g, of the toughened systems when compared to that of the neat resin system; and the decrease in T_g scaled with the content of G added in the system. Impact strength tests showed that the impact strength was improved significantly by adding G into the resin system and it increased by a factor of 13.7 for the system with 13 wt.% content of G. In addition, the toughened systems were found to yield during the impact strength test whereas brittle fracture occurred for the neat epoxy resin system; this behavior could be further confirmed by the results of scanning electron microscopy (SEM). In the shape memory behavior tests, strain fixity ratio reached as high as 98.9% for toughened systems with 7, 9, 11, 13, and 15 wt.% of G. Toughened systems also displayed changed shape recovery behavior that was comparable with that of the neat epoxy resin system during shape memory process.

Keywords

shape memory epoxy, toughening, mechanical properties, shape memory effects

Introduction

Shape memory polymers (SMPs) are polymeric smart materials which possess the ability to store and recover large strains by the application of a prescribed thermomechanical cycle in response to an external stimulus, such as temperature, electric or magnetic field, light, or pH value.[1–6] SMPs can be either thermoplastics or thermosettings with physically or chemically cross-linked network structures, permitting a rubbery plateau within a temperature range above glass transition temperature (T_g). Several polymers, including polyurethane, polynorbornene, styrene-butadiene copolymers, cross-linked polyethylene, and epoxy-based polymers, have been investigated with shape memory behaviors.[7–10] SMPs are superior in several respects, including low density and controllable activation temperature range that is related to T_g which could be tailored by the control of the molecular structure of either the main chains or pendant groups.[11]

Recently, more attention has been paid to the thermosetting-based composite SMPs deployable for space structures,[12–14] which can be folded into specific shapes when heated above T_g, launched into the preordained orbital (determined orbital in advance), and then heated to temperatures above T_g again to restore to their original shapes by virtue of shape memory effects, ultimately reducing the launch spatial volume and cost significantly.[15–17]

[1] Department of Polymer Materials and Engineering, Harbin Institute of Technology, Harbin, Heilongjiang, China
[2] National Key Laboratory of Science and Technology on Advanced Composites in Special Environments, Harbin Institute of Technology, Harbin, Heilongjiang, China
[3] Center for Composite Materials, Harbin Institute of Technology, Harbin, Heilongjiang, China
[4] Integrated Composites Laboratory (ICL), Dan F. Smith Department of Chemical Engineering, Lamar University, Beaumont, TX, USA

Corresponding author:
Yu-Yan Liu, Department of Polymer Materials and Engineering, Harbin Institute of Technology, Harbin, Heilongjiang 150001, China.
Email: liuyy@hit.edu.cn or zhanhu.guo@lamar.edu

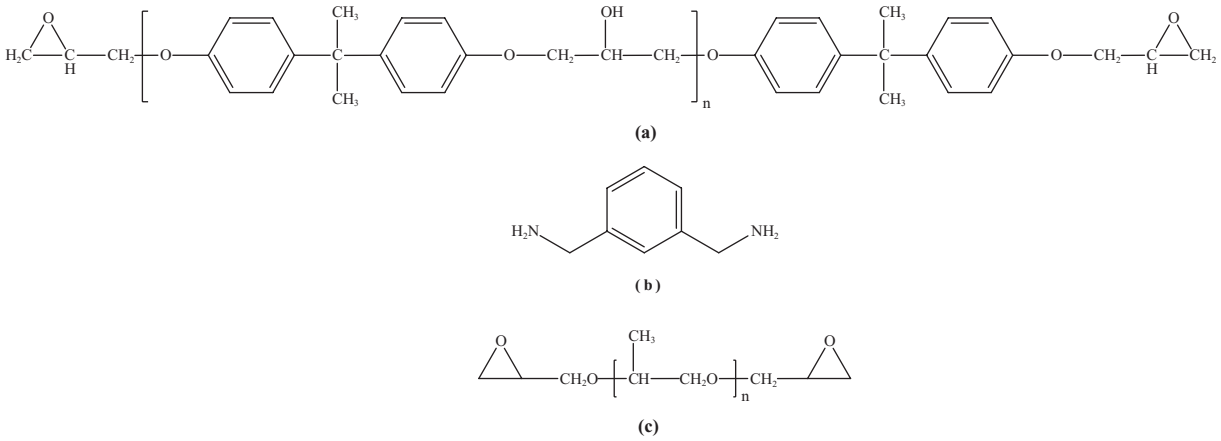

Scheme 1. Chemical structures of (a) the epoxy resin E-51, (b) the curing agent *m*-xylylenediamine and (c) the toughening agent polypropylene glycol diglycidyl ether (G), respectively.

Among the SMPs, epoxy resins are perceived as an ideal hosting thermosetting matrix of the SMP composites due to their excellent properties such as high fracture stress, specific elastic modulus, and good geometrical, thermal and environmental stabilities.[18–20] Shape memory alloy/epoxy hybrid SMP composites with large bending strength and fracture strain[21] and controllable suppressed stress intensity in the vicinity of a crack-tip[22] have been fabricated and reported. However, one main disadvantage of the epoxy-based SMPs is related to their inherent brittleness and low impact strength arising from the highly cross-linked network structure.[23,24]

To improve the toughness of epoxy, silica nanoparticles,[25] double-walled carbon nanotubes[26] or single-walled carbon nanotubes,[27] or graphene oxide[28] have been introduced to the epoxy matrix. Meanwhile, carbon nanofibers, carbon nanotubes and Fe@FeO core-shell nanoparticles have been used to improve the tensile strength of the epoxy matrix and other functionalities such as electrical conductivity and magnetic properties.[29–32] However, the poor compatibility of the epoxy matrix and the nanoparticles or nanotubes, which results in severe aggregation of the nanofillers, remains the problem.[33,34] To obtain homogenous epoxy SMPs with enhanced toughness is not trivial. In the present study, a readily commercially available polypropylene glycol diglycidyl ether (G) was evaluated as the toughening agent, and the results showed a good compatibility between G and the epoxy matrix. The effects of the toughening agent on the mechanical properties of the shape memory epoxy systems were evaluated. The shape memory effects in terms of strain fixity ratio and strain recovery ratio at different temperatures were also considered. The overall optimum content of G was studied for this epoxy resin as the polymeric matrix of SMP composites deployable in the space structures.

Materials and experimental

Materials

In the experiment, E-51, a diglycidyl ether type epoxy resin from bisphenol A with an epoxy value of 0.48–0.54, was purchased from LanXing Chemical Co., Ltd, China. The amine curing agent, *m*-xylylenediamine, was provided by Aladdin, China, and the toughening agent polypropylene glycol diglycidyl ether (G) was supplied by XiYaShiji Co., Ltd, China. The chemical structures of E-51, *m*-xylylenediamine and polypropylene glycol diglycidyl ether are shown in Scheme 1.

Preparation of epoxy SMP systems

Neat epoxy systems with a degree of curing (DC, the ratio of the number of reacted sites to the total number of reactive sites) of 60, 70, 80, 90, and 100% were prepared following the procedures in our previous study.[35] Briefly, the curing agent and toughening agent were successively added into E-51 at room temperature. The mixture was stirred for 5 min to obtain a homogenous solution. Finally, the solution was put into a rotary-vane vacuum oven for 10 min to remove the bubbles formed in the solution. The curing was carried out according to the curing procedures recommended by the company: 80°C for 2 h and 160°C for another 6 h. The pure epoxy system with a curing degree of 80%, denoted as EP-80, was found to be the most suitable system for studying because it possessed the most desirable comprehensive properties in terms of strength, toughness, and shape memory effects.[36] Therefore, investigation on the toughening of the shape memory epoxy was conducted based on EP-80. The shape memory epoxy systems with different formulas based on EP-80 are listed in Table 1 (in terms of weight percentage).

Table 1. Formulas of SMP epoxy systems.

Epoxy systems	EP-80	EPG-7	EPG-9	EPG-11	EPG-13	EPG-15
E-51 (g)	100	93	91	89	87	85
Toughening agent (g)	0	7	9	11	13	15
Curing agent (g)	13.89	13.57	13.47	13.36	13.26	13.12

Characterizations

Fourier transform infrared spectrometry tests. Fourier transform infrared spectrometry (FT-IR) tests were performed on a Nicolet-Nexus-670 Fourier transform infrared spectrometry instrument using KBr pellets in the range of 500 to 4000 cm^{-1} at a resolution of 4 cm^{-1} to investigate the interaction between the toughening agent and the epoxy resin.

Torsional braid analysis. Aromatic fibers were knitted into even braids and then were cut into short ones with a length of 7 cm. Both ends of each of the short braids were fixed on a self-made aluminum plate with the middle part well wetted by the resin mixtures prepared beforehand. Then the braids were cured according to the curing procedures recommended by the company: 80°C for 2 h and 160°C for another 6 h. Finally, the cured braid specimens were put inside a GDP-4 instrument for dynamic mechanical properties analysis (DMA). DMA is the most useful technique used to study the viscoelastic behavior of polymers where a sinusoidal stress is applied and the strain is measured to obtain the complex modulus. The dynamic mechanical properties and internal friction data were obtained, allowing for the determination of T_g of different resin systems. The tests were carried out at a heating rate of 2°C min^{-1} with a frequency of 10 Hz.

Impact strength tests. Resin systems with different content of G were cured in channeled molds and the moldings were fabricated into cylindrical specimens with a dimension of 65 mm × 0.6 mm × 0.6 mm, according to GB/T1843-1996 standard in China, which specifies the requirements of preparing unnothched plastic samples to be tested on the cantilever impact testing machine. An Instron 9250HV frame for the drop hammer impact test was adapted in this experiment, using a damping velocity of 3.5 m/s. The cantilever impact strength (the ratio of the energy absorbed by the pristine specimen to areas of its original cross section) was defined as α (kJ/m^2) and can be calculated according to Equation (1):[37]

$$\alpha = W/(h \times b) \quad (1)$$

where W is the energy absorbed by the pristine specimen (J); h is the thickness of the specimen(mm); and b is the width of the specimen (mm).

Scanning electron microscopy characterizations. The morphology and microstructure of the fracture cross-sections of the neat epoxy and toughened epoxy systems were studied using an FEI Quanta 200F system instrument.

Shape memory behavior tests. At temperature above T_g, the polymeric materials transform from a glassy state to a rubbery state and are then capable of being deformed by the application of an external stress. The stress can be stored to some extent when the polymeric materials are cooled down below T_g. $R_f(T)$ is employed to indicate the ability for the polymeric materials to hold the deformed shape, or temporary shape at a certain temperature of T, and can be calculated according to Equation (2):[38,39]

$$R_f(T) = \frac{\theta_{fixed}}{\theta_{max}} \times 100\% \quad (2)$$

where $R_f(T)$ is the strain fixity ratio at T, θ_{max} is the original bent angle, that is, 180°, and θ_{fixed} is the bent angle maintained at T.

For shape memory materials, the original shape can be restored after an appropriate thermomechanical treatment. R_r is an indicator of this recovery ability. R_r can be calculated using Equation (3):[38,39]

$$R_r(T) = \frac{\theta_{fixed} - \theta_{final}}{\theta_{fixed}} \times 100\% \quad (3)$$

where R_r (T) is the strain recovery at T; θ_{fixed} is the bent angle maintained at T; and θ_{final} is the residual bent angle after shape recovery.

The specimen (150 mm × (20 ± 0.2) mm × (2 ± 0.2) mm) was bent into an U shape of 12 mm inside diameter and the bent angle θ_{max} was normalized to 180°. The deformed specimen was cooled down and then heated again for shape memory performance evaluation.

Results and discussion

FT-IR analysis of SMP epoxy systems

Figure 1(a) and (b) shows FT-IR spectra of the cured neat epoxy resin EP-80 and toughened epoxy resin EPG-15, respectively. In Figure 1(a), the hydroxyl groups produced by the ring-opening reaction of E-51 with the amine curing agent, combined with the pendent hydroxyl group of E-51 (Scheme 1(a)) gave rise to a prominent –OH stretch peak at 3300–3400 cm^{-1}.[40] The theoretical curing degree was only 80%, therefore some epoxy groups remained unreacted in the shape memory epoxy resin system, which is verified by the stretch peak at 916 cm^{-1}.[41] In Figure 1(b), the content of E-51 was decreased when polypropylene glycol diglycidyl ether (G) was introduced to the shape memory

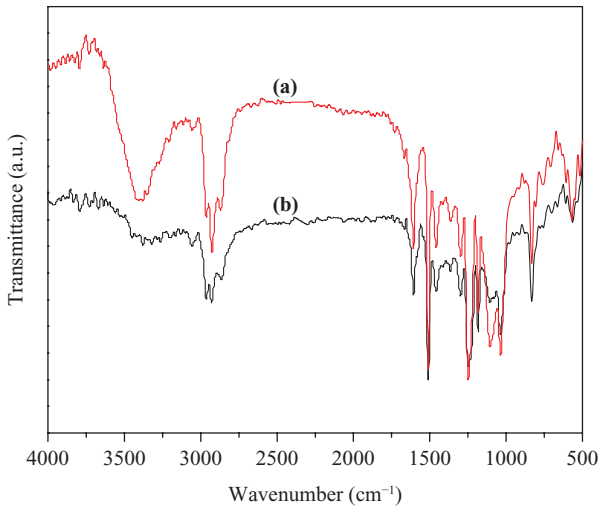

Figure 1. FT-IR spectra of (a) EP-80 and (b) EPG-15.

epoxy resin system. As aromatic epoxy groups are more active than those aliphatic epoxy groups, E-51 would react more readily with the curing agent than glycol diglycidyl ether, and part of the hydroxyl groups produced would further react with the epoxy groups, resulting in partial consumption of the hydroxyl groups. Furthermore, there are no hydroxyl groups in the polypropylene glycol diglycidyl. Therefore, the –OH stretch peak at 3300–3400 cm^{-1}, Figure 1(b), is not as obvious as the –OH stretch peak in Figure 1(a). The stretch peak at 916 cm^{-1} is attributed to those unreacted epoxy groups in the polypropylene glycol diglycidyl ether.

Torsional braid analysis of the SMP epoxy systems

Results of the torsional braid analysis (TBA) test are illustrated in Figures 2 and 3, where the logarithmic decrement Δ ($\Delta = \ln(A_1/A_2) = \ln(A_2/A_3) = \ln(A_n/A_{n+1})$, where A_n represents the amplitude of the nth oscillation of the sample). Figure 2(a) and Figure 3(a) indicate that the mechanic loss (work exhausted because of the creep phenomenon arising from the lag of strain change induced by the stress change in each cycle for the polymer materials) while $1/P^2$ in Figure 2(b) and 3(b) represents the shear modulus (the ratio of shear stress to the shear strain). Figure 2(a) and Figure 3(a) also provide information about the T_g values of the different resin systems, which are listed in Table 2.

The TBA results of EPG-15 and EP-80 (Figure 2) show the thermomechanical differences between the toughened (EPG-15) and neat resin systems (EP-80). From Figure 2(a), T_g of EPG-15 is calculated to be 51.2°C which is lower than that (94.7°C) of EP-80. This phenomenon might be attributed to the aliphatic structure and smaller molecular weight of G. However, the peak width of T_g was found to have almost the same value for EP-80 and EPG-15. The full width at half maximum of T_g peak was calculated to be 25.6°C for EPG-15 and 25.2°C for EP-80. Therefore, it can be concluded that G has little effect on the polymer chain relaxation process. From Figure 2(b), similar $1/P^2$ curves for EPG-15 and EP-80 were observed. The value of $1/P^2$ first decreased dramatically at the vicinity of T_g, and then a plateaus above T_g was observed. This is characteristic of a highly cross-linked and monophase structure, indicating that G had a good compatibility with the epoxy matrix.

Figure 3 shows the mechanic loss and stiffness change of the toughened epoxy systems with different amounts of G. The T_g value was observed to decrease with increasing G content. Values of T_g, inferred from the peak in Figure 3(a), were found to be 89.2, 72.4, 64.3, and 58.8°C for EPG-7 EPG-9, EPG-11, and EPG-13, respectively, and full width at half maximum of T_g peak was similar for these systems. Therefore, it could be inferred that the molecular interaction was weakened while the cross linking structure was not diminished by introducing G into the SMP systems.[20] It also indicates that G has a great potential in tailoring T_g of the shape memory epoxies.[18]

Impact strength tests and morphology

Table 3 and Figure 4 show the impact strength of the different toughened resin systems and the load–time curves, respectively. From Table 3, the impact strength (8.623, 10.230, 11.560, 13.688, and 13.456 kJ/m^2 for EPG-7, EPG-9, EPG-11, EPG-13, and EPG-15, respectively) was improved significantly with increasing G content and reached a maximum of 13.688 kJ/m^2 at 13 wt.% of G, which was about 13.7 times of that of the neat epoxy system (0.996 kJ/m^2). However, the impact strength began to decline in the SMPs with G loading above that critical content. There was only one peak in the curve of loan versus time for neat resin EP-80 (Figure 4(a)) indicating that the neat resin fractured directly. Interestingly, more than one peak was observed (Figure 4(b) and (c)) when G was added in the epoxy resin system, and the number of peaks and the maximum sustainable load increased with increasing the content of G, indicating the ductility of the epoxy resin after the addition of G, which was further confirmed by the following scanning electron microscopy (SEM) observations of the fracture cross-sections of the neat epoxy and the toughened epoxy system.

Figure 5 shows the SEM images of the fracture cross sections of (a) EP-80 and (b) EPG-15. The fracture section was very smooth for the cured pure EP-80, while the fracture surface became much rougher and uneven for EPG-15, This indicates that G was very effective in enhancing the toughness of the epoxy resin[42,43] and this was also observed in the nanoparticles reinforced vinyl ester resin nanocomposites[44] and carbon nanofibers-reinforced epoxy nanocomposites[30] with an enhanced tensile strength.

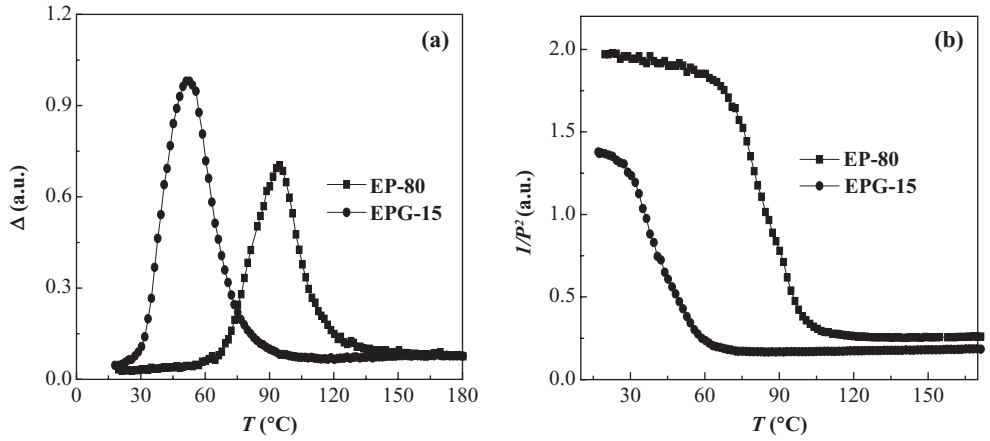

Figure 2. (a) Mechanical loss versus temperature and (b) stiffness loss versus temperature from TBA tests for neat epoxy resin EP-80 and toughened EPG-15 epoxy resin systems.

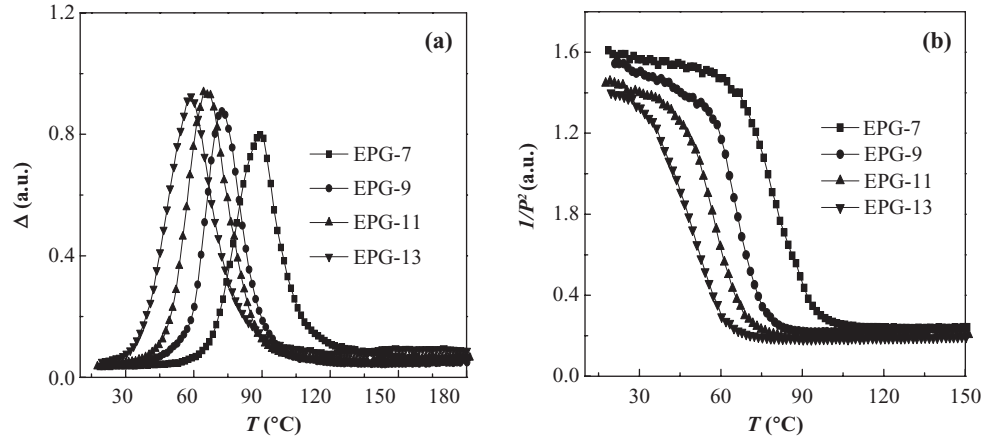

Figure 3. (a) Mechanical loss versus temperature and (b) stiffness loss versus temperature from TBA tests for the toughened systems containing G 7, 9, 11, 13%.

Table 2. T_g of different epoxy systems.

Epoxy systems	EP-80	EPG-7	EPG-9	EPG-11	EPG-13	EPG-15
T_g (°C)	94.7	89.2	74.2	64.3	57.2	51.2

Table 3. Impact strength of different epoxy systems.

Epoxy systems	EP-80	EPG-7	EPG-9	EPG-11	EPG-13	EPG-15
Impact strength (kJ/m^2)	0.996	8.623	10.230	11.560	13.688	13.456

Shape memory performance test

Shape performances of EP-80, EPG-7, EPG-9, EPG-11, EPG-13, EPG-15 and EPG-17 were studied. Each of the epoxy systems was heated to temperatures above T_g such as $T > T_g + 20 \sim 30$°C for 10 min, folded into a U shape, and cooled down to room temperature while maintaining the external force. After 5 min the bent angle, θ_{fixed}, was measured and the strain fixity ratio R_f could be calculated using Equation (3). R_f was found to be greater than 98.9%.

For each system, it was observed that the recovery happened quite slowly when θ_{fixed} was above 150° (R_r below 16.7%, Equation (3)) or below 30° (R_r above 86.3%), and the shape recovery happened rapidly when θ_{fixed} ranged from 150 to 30° (R_r below 86.3% and above 16.7%).

Figure 6 shows the recovery process of the various systems containing different amounts of G. For instance, the recovery of EP-80 began at 70°C but could not completely reach the initial condition until the temperature reached 95°C, suggesting that the recovery process started at the beginning of glass transition, at which temperature the molecular chains tended to move after having gained some external energy and gave rise to a decreased modulus. However, the recovery could not happen readily due to the significant friction between polymer molecules and comparatively weak chain motion. At higher temperature when more free volume was

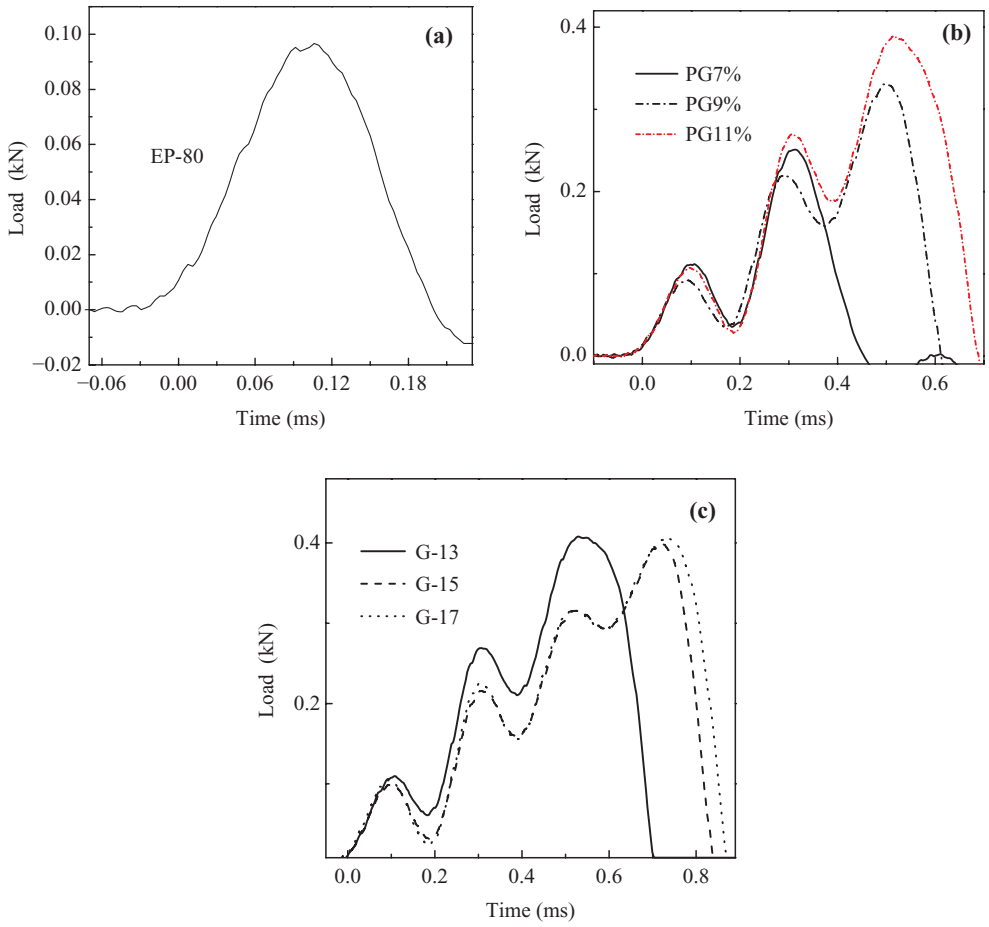

Figure 4. Load versus time of epoxy system of (a) EP-80 and (b) toughened systems containing G 7, 9, 11% and (c) toughened systems containing13, 15, 17% of G, respectively.

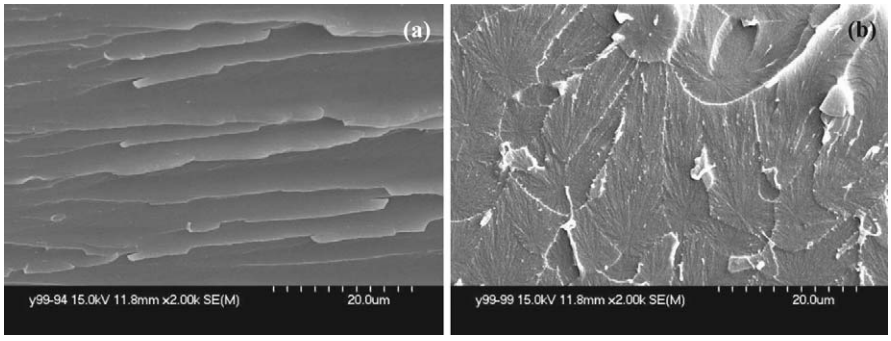

Figure 5. SEM images of (a) EP-80 and (b) EPG-15, respectively.

available, the frozen chains were set free and R_r began to increase subsequently. When the temperature reached 95°C the extrapolated terminal temperature of the glass transition, and the internal friction were reduced dramatically and the specimen was able to recover to its original shape completely, driven by released frozen strain which was stored in the polymer matrix during the shape deformation.

It was also observed that the recovery temperature shifted from 70 to 50°C with increasing G in the systems, which implied that G participated in reducing the cross-linking density. Hence, molecular chains can move with comparatively less energy requirement and render the deformed shape recovery at a lower temperature.

Conclusions

The toughening of SMP epoxy resin using polypropylene glycol diglycidyl ether (G) was studied. Various

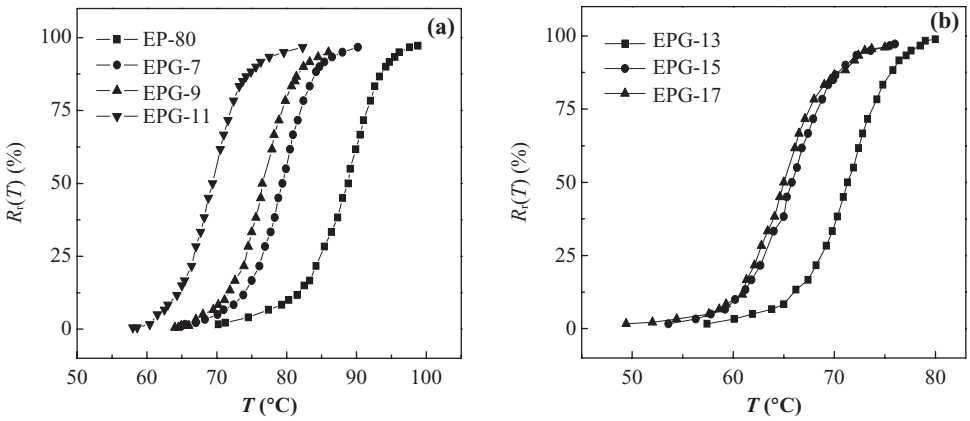

Figure 6. Strain recovery ratio of (a) EP-80, EPG-7, EPG-9 and EPG-11 and (b) EPG-13, EPG-15 and EPG-17, respectively.

characterizations methods including TBA test, impact strength test, DMA and shape memory effects test were employed to investigate the effects of the toughening agent on the epoxy resin SMPs. The results showed that G had a good compatibility with the epoxy matrix. The toughness of the epoxy resin SMP could be improved significantly with a prime content of 13 wt.% of G, although a slight decrease in the T_g value of the toughened epoxy systems could be brought due to the aliphatic structure and lower molecular weight of G. The shape memory tests demonstrated that toughened systems such as EPG-7, EPG-9, EPG-13 and EPG-15 possess the ability of shape memory with the strain fixity ratio being as high as 98.9%. The toughening epoxy systems with G can recover to their original shapes more easily at lower temperatures.

Funding

This work was financially supported by the Program for Harbin city science and technology innovation talents of special fund project (2012RFXXG091) and Pre-research Fund Project of National Defense. Z. Guo appreciates the support from NSF (CMMI 10-30755).

References

1. Liu C, Qin H and Mather P. Review of progress in shape-memory polymers. *J Mater Chem* 2007; **17**: 1543–1558.
2. Xie T, Xiao X and Cheng YT. Revealing triple shape memory effect by polymer bilayers. *Macromol Rapid Commun* 2009; **30**: 1823–1827.
3. Lendlein A, Jiang H, Jünger O, et al. Light-induced shape-memory polymers. *Nature* 2005; **434**: 879–882.
4. Jiang H, Kelch S and Lendlein A. Polymers move in response to light. *Adv Mater* 2006; **18**: 1471–1475.
5. Huang W, Yang B, An L, et al. Water-driven programmable polyurethane shape memory polymer: Demonstration and mechanism. *Appl Phys Lett* 2005; **86**: 114105–114105–3 .
6. Ahmad M, Luo J, Singh D, et al. Shape memory effect and thermomechanical properties of shape memory polymer fabric composite in tension mode. *World J Eng* 2012; **9**: 85–92.
7. Ratna D and Karger-Kocsis J. Recent advances in shape memory polymers and composites: a review. *J Mater Sci* 2008; **43**: 254–269.
8. Chung YC, Shim YS and Chun BC. Effect of glucose cross-linking on thermomechanical properties and shape memory effect of PET PEG copolymers. *J. Appl. Polym. Science* 2008; **109**: 3533–3539.
9. Liu C, Chun SB, Mather PT, et al. Chemically cross-linked polycyclooctene: synthesis, characterization, and shape memory behavior. *Macromolecules* 2002; **35**: 9868–9874.
10. Merline J, Reghunadhan Nair C, Gouri C, et al. Poly (urethane-oxazolidone): Synthesis, characterisation and shape memory properties, *Eur Polym J* 2007; **43**: 3629–3637.
11. Yakacki CM, Shandas R, Safranski D, et al. Strong, tailored, biocompatible shape-memory polymer networks. *Adv Funct Mater* 2008; **18**: 2428–2435.
12. Lake MS and Campbell D. The fundamentals of designing deployable structures with elastic memory composites. *IEEE Aerospace Conference* 2004; **4**: 2745–2756.
13. Lan X, Liu Y, Lv H, et al. Fiber reinforced shape-memory polymer composite and its application in a deployable hinge. *Smart Mater Struct* 2009; **18**: 024002.
14. Gall K, Dunn ML, Liu Y, et al. Shape memory polymer nanocomposites. *Acta Mater* 2002; **50**: 5115–5126.
15. Campbell D, Lake MS, Scherbarth MR, et al. Elastic memory composite material: an enabling technology for future furlable space structures. In: *46th AIAA/ASME/ASCE/AHS/ASC Struct., Struct. Dyn., Mater. Conf.*, 2005; pp. 1–12.
16. Mileti S, Guarrera G, Marchetti M, et al. The FLECS expandable module concept for future space missions and an overall description on the material validation. *Acta Astronaut* 2006; **59**: 220–229.
17. Mather PT, Luo X and Rousseau IA. Shape memory polymer research. *Annu Rev Res* 2009; **39**: 445–471.
18. Xie T and Rousseau IA. Facile tailoring of thermal transition temperatures of epoxy shape memory polymers. *Polymer* 2009; **50**: 1852–1856.

19. Leonardi AB, Fasce LA, Zucchi IA, et al. Shape memory epoxies based on networks with chemical and physical cross-links. *Eur Polym J* 2010; **3**: 362–369
20. Liu Y, Han C, Tan H, et al. Thermal, mechanical and shape memory properties of shape memory epoxy resin. *Mater Sci Eng: A* 2010; **527**: 2510–2514.
21. Tian B, Chen F, Tong Y, et al. Bending properties of epoxy resin matrix composites filled with Ni–Mn–Ga ferromagnetic shape memory alloy powders. *Mater Lett* 2009; **63**: 1729–1732.
22. Shimamoto A, Zhao H and Azakami T. Active control for stress intensity of crack-tips under mixed mode by shape memory TiNi fiber epoxy composites. *Smart Mater Struct* 2007); **16**: 13–21.
23. Liu Y, Gall K, Dunn ML, et al. Thermomechanical recovery couplings of shape memory polymers in flexure. *Smart Mater Struct* 2003; **12**: 947–954.
24. Liu Y, Gall K, Dunn ML, et al. Thermomechanics of shape memory polymers: uniaxial experiments and constitutive modeling. *Int J Plast* 2006; **22**: 279–313.
25. Hsieh T, Kinloch A, Taylor A, et al. The effect of silica nanoparticles and carbon nanotubes on the toughness of a thermosetting epoxy polymer. *J Appl Polym Sci* 2011; **119**: 2135–2142.
26. Gojny F, Wichmann M, Kopke U, et al. Carbon nanotube-reinforced epoxy-composites: enhanced stiffness and fracture toughness at low nanotube content, *Compos Sci Technol* 2004; **64**: 2363–2371.
27. González-Domínguez JM, Ansón-Casaos A, Díez-Pascual AM, et al. Solvent-free preparation of high-toughness epoxy− SWNT composite materials. *ACS Appl Mater Interfaces* 2011; **3**: 1441–1450.
28. Bortz DR, Heras EG and Martin-Gullon I. Impressive fatigue life and fracture toughness improvements in graphene oxide/epoxy composites. *Macromolecules* 2011; **45**: 238–245.
29. Zhu J, Wei S, Yadav A, et al. Rheological behaviors and electrical conductivity of epoxy resin nanocomposites suspended with in-situ stabilized carbon nanofibers. *Polymer* 2010; **51**: 2643–2651.
30. Zhu J, Wei S, Ryu J, et al. In situ stabilized carbon nanofiber (CNF) reinforced epoxy nanocomposites. *J Mater Chem* 2010; **20**: 4937–4948.
31. Zhu J, Wei S, Ryu J, et al. Magnetic epoxy resin nanocomposites reinforced with core-shell structured Fe@FeO nanoparticles: fabrication and property analysis, *ACS Appl Mater Interfaces* 2010; **2**: 2100–2107.
32. Wang Z, Yang X, Wang Q, et al. Epoxy resin nanocomposites reinforced with ionized liquid stabilized carbon nanotubes. *Int JSmart Nano Mater* 2011; **2**: 176–193.
33. Hollertz R, Chatterjee S, Gutmann H, et al. Improvement of toughness and electrical properties of epoxy composites with carbon nanotubes prepared by industrially relevant processes. *Nanotechnol* 2011; **22**: 125702–125710.
34. Hsieh T, Kinloch A, Taylor A, et al. The effect of carbon nanotubes on the fracture toughness and fatigue performance of a thermosetting epoxy polymer. *J Mater Sci* 2011; **46**: 7525–7535.
35. Liu F. *Study on Preparation of Shape Memory Epoxy Resin and Properties of Its Composites*. Master dissertation, Harbin Institute of Technology, 2009.
36. Gurrappa I and Binder L. Electrodeposition of nanostructured coatings and their characterization – a review. *Sci Technol Adv Mater* 2008; **9**: 043001–043011.
37. KaelbleJohn DH. *Physical Chemistry of Adhesion*. New York: Wiley & Sons, 1971.
38. Li F and Larock RC. New soybean oil–styrene–divinylbenzene thermosetting copolymers. v. shape memory effect. *J Appl Polym Sci* 2002; **84**: 1533–1543.
39. Lin J and Chen L. Study on shape memory behavior of polyether based polyurethanes. I. Influence of the hard segment content. *J Appl Polym Sci* 1998; **69**: 1563–1574.
40. Shishmakov A, Erankin S, Mikushina YV, et al. Activated carbon and carbon-oxide composite materials derived from powdered cellulose. *Russ J Appl Chem* 2010; **83**: 307–311.
41. Sánchez-Soto M, Pages P, Lacorte T, et al. Curing FTIR study and mechanical characterization of glass bead filled trifunctional epoxy composites. *Compos Sci Technol* 2007; **67**: 1974–1985.
42. Levita G. Matrix ductility and toughening of epoxy resins. *Adv Chem Ser* 1989; **222**: 93–118.
43. Hodgkin J, Simon G and Varley R. Thermoplastic toughening of epoxy resins: a critical review. *Polym Adv Technol* 1998; **9**: 3–10.
44. Guo Z, Pereira T, Choi O, et al. Surface functionalized alumina nanoparticle filled polymeric nanocomposites with enhanced mechanical properties. *J Mater Chem* 2006; **16**: 2800–2808.